

Solvent Interactions of Halophilic Malate Dehydrogenase[†]

Christine Ebel,^{*,‡} Lionel Costenaro,^{‡,§} Mihaela Pascu,^{‡,||} Pierre Faou,^{‡,⊥} Blandine Kernel,[‡]
Flavien Proust-De Martin,^{‡,#} and Giuseppe Zaccai^{‡,‡}

Laboratoire de Biophysique Moléculaire, Institut de Biologie Structurale, UMR 5075 CEA-CNRS-UJF, 41 rue Jules Horowitz,
38027 Grenoble, France, and Institut Laue Langevin, 6 rue Jules Horowitz, BP 156, 38042 Grenoble Cedex 9, France

Received March 18, 2002; Revised Manuscript Received August 30, 2002

ABSTRACT: Malate dehydrogenase from the extreme halophilic *Haloarcula marismortui* (*Hm* MalDH) is an acidic protein that is unstable below molar salt concentrations. The solvated folded protein was studied by small-angle neutron scattering in solvents containing salt: NaCl, NaCH₃CO₂, KF, NH₄Cl, NH₄CH₃CO₂, (NH₄)₂SO₄, MgCl₂, and MgSO₄. It was found that the global solvent interactions depend mainly on the nature of the cation. Complementary mass density measurements in MgCl₂, NaCl, NaCH₃CO₂, and (NH₄)₂SO₄ allowed determining the partial molal volumes of the protein, which were found to increase slightly with the salt, and the preferential salt binding parameters for each solvent condition. These are strongly dependent on the cation type and salt concentration. *Hm* MalDH can be modeled as an invariant particle binding 4100 water molecules in MgCl₂ and 2000 ± 200 in NaCl, NaCH₃CO₂, or (NH₄)₂SO₄. The number of salt molecules associated to the particle decreases from about 85 to 0 in the order MgCl₂ > NaCl = NaCH₃CO₂ > (NH₄)₂SO₄. Alternatively, we considered exchangeable sites for water and salt with the effects of solvent nonideality. It does not change the description of the solvent interactions. Solvent anions act on *Hm* MalDH stability through a limited number of strong binding sites, as those seen at the interfaces of *Hm* MalDH by crystallography. Cations would act through some strong and numerous weak binding sites defined on the folded protein, in possible addition to nonspecific hydration effects.

Extreme halophilic Archaea such as *Haloarcula marismortui* require for their optimal growth salt concentrations close to saturation and are found in environments such as the Dead Sea. To counterbalance the external osmotic pressure, they accumulate in their cytoplasm salt concentrations close to saturation, mainly KCl. All their enzymatic machinery is adapted to high salt concentration. The question of protein adaptation to high salt has been discussed in recent reviews (1, 2). One of the main characteristics of halophilic proteins is their instability at low salt, typically below 2 M KCl. Their amino acid composition is characterized by a high content of acidic residues (3, 4). The global solvation of glyceraldehyde-3-phosphate dehydrogenase from *Haloarcula vallismortis*, elongation factor Tu, and malate dehydrogenase (*Hm* MalDH)¹ from *Haloarcula marismortui* (*Hm*) have been quantified in high KCl and NaCl (5–8). For these three

halophilic proteins, the solvation shell can be described as composed of 0.2–0.4 g of water and 0.1–0.2 g of salt per gram of protein. If the water content is similar to the hydration of nonhalophilic proteins, the amount of salt appears to be much larger. It was proposed that a network of hydrated ions interacting with carboxylates in patches on the protein surface would stabilize the folded *Hm* MalDH in high KCl or NaCl (9). In the crystallographic structure at 1.9 Å resolution of *Hm* 2Fe–2S Ferredoxin, three phosphate ions and only six potassium ions were found, while numerous tightly bound water molecules were described (10). Crystallographic studies of wild type (at 2.9 Å resolution) and a mutant (at 2.6 Å resolution) of *Hm* MalDH allowed to assign only two sodium and four chloride ions as part of four salt-bridge clusters localized at the interfaces between subunits (11). Thus, the very large salt solvation inferred from solution studies on *Hm* MalDH cannot be detected at high resolution. It can be due to the disorder of the solvent molecules. Similarly, univalent cations are hardly detected in nucleic acids crystals, while they are described by molecular dynamics (12, 13). It is possible, however, that the solvation shell of the halophilic protein does not contain such a large amount of salt in the solvent conditions used for crystallization, as suggested in a solution study on *Hm* MalDH in 1.5 M K-phosphate (9). Also, from thermodynamic kinetic activation parameters at various temperatures, the stabilization of halophilic proteins could be achieved by different

[†] This work was supported by the CNRS, CEA, and CNES (Décision 793/2001/CNES/8860).

* Corresponding author. Tel: 33 (0)4 38 78 96 38. Fax: 33 (0)4 38 78 54 94. E-mail: Christine.Ebel@ibs.fr.

[‡] Laboratoire de Biophysique Moléculaire, Institut de Biologie Structurale.

[§] Present address: Biological Chemistry Department, John Innes Centre, Colney Lane, Norwich NR4 7UH, United Kingdom.

^{||} Present address: Medicine and Pharmacy University, Department of Biophysics and Radiopharmacy, 6600 Iasi, Romania.

[⊥] Present address: Institut für Biochemie und Molekularbiologie der Universität Freiburg, Hermann-Herder-Strasse 7, D 79104 Freiburg, Germany.

[#] Present address: Scuola Internazionale Superiore di Studi Avanzati, 2-4, Via Beirut 34013 Trieste, Italy.

[‡] Institut Laue Langevin.

¹ Abbreviations: *Hm* MalDH, malate dehydrogenase from *Haloarcula marismortui*; SANS, small-angle neutron scattering.

mechanisms, depending of the salt nature: for example, salt binding in KCl and NaCl, or hydrophobic effect in ammonium sulfate or high K-phosphate (14).

The relative effects of the anions and cations on *Hm* MalDH stability were evaluated in a comparative study of various salts (15) and found essentially to superimpose, as generally found for salts in the molar range. If an anion or a cation was very stabilizing, the effect of the salt ion of opposite charge was very limited. Anions of high charge density were always the most efficient to stabilize the folded form, in accordance with their classifications in the Hofmeister series. Cations of highest charge density stabilized also in the more efficient way the folded form of *Hm* MalDH (with, in some cases, high-salt unfolding). The salt effects on protein stability are related to different interactions of the folded and unfolded protein with the solvent components. Solvent interactions arise from specific water or ion binding or nonspecific mechanisms. One of the latter is linked to the surface tension of the solvent (an increase of the surface tension corresponds to water accumulation at the surface of the protein), which explains in part the general effect of salts on the conformation of the macromolecules. For *Hm* MalDH, the qualitative analysis of the stabilizing efficiency of the salts suggested that nonspecific effects induced by surface tension were of minor importance. Specific weak or strong interactions of the ions for sites specific of the folded protein would be of importance. They would determine the large amount of salt previously determined in *Hm* MalDH solvation shell in NaCl or KCl.

Different mechanisms of stabilization—surface tension effect, weak or strong ion binding—would determine a different solvation. To have insights into their relative importance for *Hm* MalDH, we measure here in a variety of salts the neutron-scattering length density contrast between the solvated *Hm* MalDH and the bulk solvent, by small-angle neutron scattering (SANS). With complementary mass density measurements, we quantify the partial specific volumes and the preferential salt binding parameters of *Hm* MalDH in selected solvents. The solvent salt concentrations, the pH value of 8.2, and the relatively low temperature (5°C) were selected for long-term protein stabilization (15, 16). Thus, the experiments presented below concern only the folded native form of *Hm* MalDH.

THEORETICAL BACKGROUND

\bar{V}_i , M_i , and m_i are the partial molal volume, molar mass, and molality (mole/kg of water) of the species or component i . Its neutron scattering length density b_i is calculated from tabulated data (17). Temperature is constant, and subscript T omitted. The subscripts μ and m signify constant chemical potentials of all diffusible components and constant molalities of all components except the derived one, respectively.

Definition of the Components. All components, water (component 1, the main solvent), macromolecule (component 2), and salt (component 3, the cosolvent), are electro neutral combinations of chemical species (18, 19). The salt is composed of ν_+ cations X of charge $+z_+$ and ν_- anions Y of charge $-z_-$. The macromolecule is the polypeptide chains plus Z/z_+ counterions required for its electro neutrality (here, $|Z| = 156$ for *Hm* MalDH tetramer, Z/z_+ is 156 singly charged cation counterions or 78 for doubly charged ones).

Hm MalDH monomer consists of 303 residues; the molar mass for the polypeptide part is 130 552 g/mol for the tetramer.

The tabulated mean ionic activity coefficient γ_{\pm} characterizes the solvent salt nonideality. Considering $\nu = \nu_+ + \nu_-$, $Q = (\nu_+^{\nu_+} \nu_-^{\nu_-})^{1/\nu}$, the activity of the salt and the mean ionic activity in the molal scale, a_3 and a_{\pm} , respectively, are related as follow: $a_3 = a_{\pm}^{\nu} = (Qm_3\gamma_{\pm})^{\nu}$. The tabulated osmotic coefficient ϕ characterizes the solvent water nonideality. It is the ratio of the actual osmotic pressure to the osmotic pressure that would be obtained in the ideal diluted case with $-\ln A_1 = \nu m_3/m_1$, where A_1 is the water activity in the mole fraction scale. Tabulated mean ionic activity and osmotic coefficients of the solvent salts can reasonably be used in the present study because the perturbation related to the presence of the protein is neglected at infinite protein dilution extrapolation.

The Partial Molal Volumes. The partial molal volumes of the components i (in mL/mol) are defined as

$$\bar{V}_i = (\partial V_m / \partial m_i)_{m,P} \quad (1)$$

V_m is the volume of the solution corresponding to 1 kg of water (principal solvent). \bar{V}_i relates the increase of the volume of the solution when the component i is added, while the concentrations of all other components are maintained constant. It can be obtained from density measurements using the pure dried or solubilized in pure water component since requiring controlled molalities of all components. The partial molal volumes of salts are thus obtained from eq 1, after trivial conversion from density tables. In the case of a polyelectrolyte macromolecule, densimetry is extremely difficult since it requires the addition to the solvent of just the polyelectrolyte and its counterions (component 2), without any modification in the solvent composition. A protocol requiring extensive dialysis against water was used for nucleic acids (8, 20). In the case of *Hm* MalDH, the protein would denature in an essentially irreversible way. We will use complementary mass density and small-angle neutron scattering performed at constant chemical potentials for the determination of \bar{V}_2 .

The Chemical Potential of the Components upon Species Dissociation. The chemical potential μ_i of the component i can be related to the molalities m_k of the related species k and to the excess chemical potential β_i . Considering the dissociation of the Z/z_+ counterions and the macromolecule as well as of the $X_{\nu+}:Y_{\nu-}$ salt

$$\mu_2 = \mu_2^{\circ} + N_A kT \ln m_2 + (Z/z_+) N_A kT \ln (\nu_+ m_3 + (Z/z_+) m_2) + N_A kT \beta_2 \quad (2)$$

$$\mu_3 = \mu_3^{\circ} + \nu_+ N_A kT \ln (\nu_+ m_3 + (Z/z_+) m_2) + \nu_- N_A kT \ln (\nu_- m_3) + N_A kT \beta_3 \quad (3)$$

Two remarks can be made. First, the use of the molality units (mol/kg of water) in these expressions has the advantage that water is not expressed explicitly. Second, the ideal state considers here the complete dissociation of the components. The consequences of the ion dissociation in eq 2 will be referred as the Donnan terms—or Donnan effects. Any incomplete dissociation will appear in the β_i terms as salt binding.

The Preferential Binding Parameter $(\partial m_3/\partial m_2)_\mu$. The preferential salt binding parameter $(\partial m_3/\partial m_2)_\mu$ is considered as experimentally indistinguishable from $(\partial m_3/\partial m_2)_{\mu 3}$ (23), which is rigorously expressed as

$$(\partial m_3/\partial m_2)_{\mu 3} = (\partial \mu_2/\partial m_3)_m / (\partial \mu_3/\partial m_3)_m = -a_{23}/a_{33} \quad (3)$$

with

$$a_{ij} = 1/RT(\partial \mu_i/\partial m_j)_{m,P} \quad (4)$$

In the present study, $Z/z_{+}m_2 \ll \nu_{+}m_3$, and a_{23} and a_{33} are

$$a_{23} = (Z/z_{+})/m_3 + \partial \beta_2/\partial m_3 = a_{23}^D + a_{23}^I \quad (5a)$$

$$a_{33} = (\nu_{+} + \nu_{-})/m_3 + \partial \beta_3/\partial m_3 \quad (5b)$$

a_{33} can be expressed with the tabulated mean ionic activity coefficients: $a_{33} = \nu/m_3 + (\partial \gamma_{\pm}/\partial m_3)\nu/\gamma_{\pm}$. The first term a_{23}^D in eq 5, related to the dissociation of the macromolecule, is the Donnan contribution in the preferential binding parameter, $E_3 = -a_{23}^D/a_{33}$. Neglecting the nonideality of the salt, it reduces to

$$E_3 = -Z/\nu z_{+} \quad (6)$$

The dissociation of the component 2 and 3 (Donnan effect) appears as a negative salt binding (see below).

Interpretation of the Values of $(\partial m_3/\partial m_2)_\mu$ in Terms of a Solvation Shell. The preferential salt binding parameter is a measurable value (see Material and Methods). It corresponds to the hypothetical number of moles of salt that would have to be added (or subtracted) with the introduction of 1 mol of the macromolecular component 2 in order to maintain constant the chemical potentials of solvent components, the concentration of water being fixed. $(\partial m_3/\partial m_2)_\mu$, which can be positive or negative, does not represent the actual salt binding. For example, water and salt strongly bound to the protein in the same ratio than that of the bulk solvent (m_3/m_1) would not change the chemical potential of the solvent. In addition, water binding is indistinguishable from salt removal, and inversely. Considering the perturbed solvent as composed of N_1 moles of water and N_3 moles of salt per mole of protein, the preferential binding parameter is

$$(\partial m_3/\partial m_2)_\mu = (N_3 - E_3) - N_1(m_3/m_1) \quad (7)$$

It can be easily understood that the numbers of bound water and salt molecules cannot be determined from one solvent-condition measurement, since one value of $(\partial m_3/\partial m_2)_\mu$ is related to an infinity of mathematical solutions (N_1, N_3). The knowledge of $(\partial m_3/\partial m_2)_\mu$ as a function of salt concentration in the solvent allows determining N_1 and N_3 within the framework of reasonable models, which are described below and schematized in Figure 1.

Interpretation of the Values of $(\partial m_3/\partial m_2)_\mu$ in Terms of an Invariant Particle. When a set of experimental data obtained at different salt concentrations (i.e., m_3/m_1 ratios) can be fitted linearly by eq 7, the particle can be described as an invariant particle, i.e., with constant $(N_3 - E_3)$ and N_1 values over the salt-concentration range of investigation (21, 22). N_3 and N_1 can be interpreted as a number of infinitively strongly bound salt and water molecules, respectively.

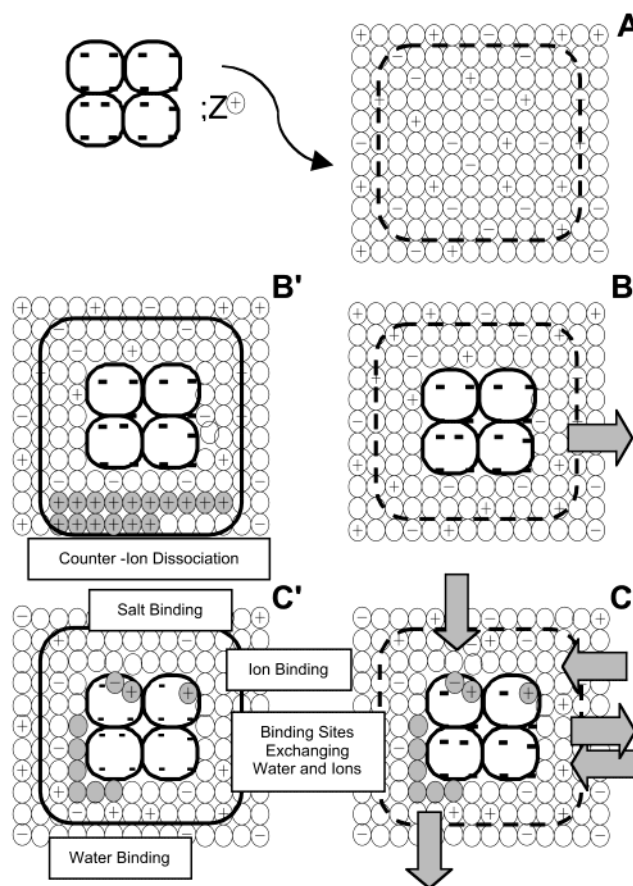


FIGURE 1: Schematic representation of the effect of counterion dissociation and water and salt binding on the preferential salt binding parameter. A: The protein, represented as a tetramer with Z negative charges, is introduced with Z monovalent cations in the solvent, consisting of water (O), the same cation (+), and anion (-). The dashed lines in panels A, B, and C represent a dialysis bag. The continuous lines in panels B' and C' indicate constant molalities of the solvent water and salt. The consequences of the events described in panels B' and C' in term of salt fluxes (in the hypothesis that there is no flux of water) accompanying the introduction of the protein in experiments performed at constant chemical potentials of the solvent water and salt are indicated in panels B and C with gray arrows. The dissociation of the polyelectrolytes (Donnan effect) leads to an increase in the concentration of cations in the solvent in panel B'. Strong water binding and salt (or ions) binding in panel C' increase the solvent concentrations of salt and water, respectively. An exiting flux of salt in the dialysis experiment corresponds to $(\partial m_3/\partial m_2)_\mu < 0$. It can be the consequence of counterion dissociation panel B, or of the presence of strong water binding panel C. An incoming flux of salt corresponds to $(\partial m_3/\partial m_2)_\mu > 0$. It is related to salt or ion binding in panel C. In the case of solvent binding sites exchanging water and ions, the consequence on the solvent composition in panel C' depends on the statistical occupancy of the binding sites and of the solvent composition: it is a solvent composition dependent combination of water and ion binding. The corresponding fluxes in panel C, and thus the sign of $(\partial m_3/\partial m_2)_\mu$, depend on the solvent composition and value of the solvent exchange equilibrium constant of the binding sites.

Interpretation of the Values of $(\partial m_3/\partial m_2)_\mu$ in Terms of Independent Solvent Exchangeable Binding Sites. Alternatively, Schellman has considered an other simple model where water and ions of the solvent are exchanged on a number N_b of identical independent solvent binding sites. Two remarks have to be made. First, anions and cations of the solvent cannot move in an independent way, since the system is always electroneutral. The N_3 moles of salt

considered in the preceding paragraph are equivalent to ν_+N_3 moles of cations and ν_-N_3 moles of anions. Here, ions of mean charge (\pm) are considered. The protein has N_b binding sites (b) occupied either by one molecule of water (b:1) or one ion (b: \pm) and characterized by a unique exchange equilibrium constant K_b . The second remark concerns the units used. A description of equilibrium involving water in the molality unit would be excessively complex. K_b can be more easily defined in the molar fraction activity scale (23–25):

$$K_b = [b:\pm]A_1/[b:1]A_{\pm} \quad (8)$$

$(\partial m_3/\partial m_2)_\mu$ is related to the salt binding parameter $(\partial m_3/\partial m_b)_\mu$ of the N_b binding sites (b) (m_b is the molality of the binding sites), which depends on K_b and solvent composition through the activities A_1 , A_{\pm} , and A_3 :

$$(\partial m_3/\partial m_2)_\mu = N_b(\partial m_3/\partial m_b)_\mu = N_b \partial \ln(A_1 + K_b A_{\pm})/\partial \ln A_3 \quad (9)$$

We have derived this equation here for the general case of salts, as was done previously for monovalent salt or neutral cosolvent (23, 25). The activities $A_1 = f_1\chi_1$ and $A_{\pm} = f_{\pm}\chi_{\pm}$ are related to the mole fractions χ_1 , χ_3 , and χ_{\pm} , defined by $\chi_1 = m_1/(m_1 + \nu m_3)$, $\chi_3 = m_3/(m_1 + \nu m_3)$, and $\chi_{\pm} = Q\chi_3$, with $Q = (\nu_+^{\nu_+}\nu_-^{\nu_-})^{1/\nu}$. The activity coefficients of water and solute in the mole fraction scale, f_1 and f_{\pm} respectively, are obtained using tabulated mean ionic activity and osmotic coefficients γ_{\pm} and ϕ at 25 °C (26): $f_1 = \exp(-\nu\phi m_3/m_1)/\chi_1$; $f_{\pm} = \gamma_{\pm}/\chi_1$. We use the operational binding constant $K'_b = Q(f_{\pm}/f_1)K_b$ to obtain

$$(\partial m_3/\partial m_b)_\mu = ((K'_b/\nu) - 1)(m_3/m_1)/(1 + K'_b(m_3/m_1)) \quad (10)$$

Despite the (relative) complexity due to the consideration of mean charge ions (\pm) and solvent nonideality, the molar fraction scale provides meaningful information from eq 10. Thus, a site with a value $K'_b = \nu$ is chemically indifferent for salt or water since it provides a null value of the preferential binding parameter. An infinite preference of the binding site for the ionic species gives a maximum value for $(\partial m_3/\partial m_b)_\mu$ of $1/\nu$, so that ν ionic binding sites (ν is the number of ions provided by one salt) correspond logically to one binding site for component 3 in eq 7: $N_b = \nu N_3$.

MATERIAL AND METHODS

Sample Preparation. *Hm* MalDH was overexpressed in *E. coli* and purified according to the protocol of Cendrin et al. (27). All salt solutions contained 50 mM Tris-HCl, pH 8.2. *Hm* MalDH was stocked in 4 M NaCl at 4 °C. Before SANS or density experiments, it was eluted through a gel filtration column (Superose 12 HR 10–30 from Pharmacia) and reconcentrated on microconcentrators (Centricon 30 from Amicon) prior to extensive dialysis. Protein concentration was measured by UV spectroscopy before the measurements (1 unit of optical density at 280 nm corresponds to 6.51 μ M, 6).

Small-Angle Neutron Scattering Experiments. Samples were contained in 1.00 mm rectangular quartz cuvettes at 5 °C. Scattering curves were recorded using a wavelength λ of 10 Å, a collimation of 2.5 m, and a sample detector

distance of 2.8 m on the instrument D11 of the “Institut Laue Langevin” (28). The Guinier approximation

$$\ln I(q) = \ln I(0) - q^2 R_g^2/3 \quad (11)$$

was used to calculate the radius of gyration R_g of the scattering-density contrast and the forward intensity $I(0)$, in a $R_g q$ range of 0.4–1.3, where $q = 4\pi \sin \theta/\lambda$ and θ is half the scattering angle (29). The protein concentration was typically 5 mg/mL. In MgCl₂, NaCl, NaCH₃CO₂, (NH₄)₂SO₄, and KF, measurements at sample–detector distance of 1.2 m were also performed in order to check the scattering levels of solvent and sample at high angles, and $I(0)$ and R_g were extrapolated at zero protein concentration from measurements at typically 6, 12, and 20 mg/mL, as described in refs 30 and 31. The neutron scattering length density increment at constant chemical potential of solvent components, $(\partial \rho_N/\partial C_2)_\mu$, in centimeters per mole of protein, was derived from the normalized scattering intensity $I(0)$ as described previously (32, 33, 8):

$$I(0) = 1/N_A C_2 (\partial \rho_N/\partial C_2)_\mu^2 \quad (12)$$

N_A being Avogadro’s number and C_2 the protein concentration in moles per milliliter.

Density Measurements. The density increments at constant chemical potential of solvent components, $(\partial \rho/\partial C_2)_\mu$, were obtained after extensive dialysis from the measurements of the density ρ and ρ° of the protein solution at typically 5 mg/mL and of the solvent, respectively, on a PAAR DMA 60 density-meter equipped with a 100 μ L DMA 601M cell thermostated at 5 °C, using a protocol described in ref 6

$$(\partial \rho/\partial C_2)_\mu = ((\rho - \rho^\circ)/C_2)_\mu \quad (13)$$

Determination of Salt Binding Parameters and Partial Specific Volumes of *Hm* MalDH. $(\partial \rho/\partial C_2)_\mu$ and $(\partial \rho_N/\partial C_2)_\mu$ can be expressed as function of the partial molal volume of component 2, \bar{V}_2 , and the salt binding parameter $(\partial m_3/\partial m_2)_\mu$:

$$(\partial \rho/\partial C_2)_\mu = (M_2 - \rho^\circ \bar{V}_2) + (\partial m_3/\partial m_2)_\mu (M_3 - \rho^\circ \bar{V}_3) \quad (14)$$

$$(\partial \rho_N/\partial C_2)_\mu = (b_2 - \rho_N^\circ \bar{V}_2) + (\partial m_3/\partial m_2)_\mu (b_3 - \rho_N^\circ \bar{V}_3) \quad (15)$$

ρ_N° is the neutron scattering length density of the solvent. \bar{V}_2 and $(\partial m_3/\partial m_2)_\mu$ can be graphically interpolated (8).

RESULTS

SANS: The Radius of Gyration. The Guinier plots (not shown) indicate an homogeneous material. The radius of gyration R_g values derived at about 5 mg/mL (eq 11) or extrapolated at zero protein concentration do not vary significantly with the salt concentration. Thus, we give here the mean value for each salt series: 30.6 Å in NaCl; 29.6 Å in NaCH₃CO₂; 31 Å in NH₄Cl; 30.4 Å in NH₄CH₃CO₂; 30.9 Å in (NH₄)₂SO₄; 32 Å in MgCl₂; 30.2 Å in MgSO₄; 31.8 Å in KF. They are always close to 31 ± 1 Å and consistent with the tetramer structure of *Hm* MalDH.

SANS: Neutron Scattering Length Density Increment $(\partial \rho_N/\partial C_2)_\mu$. The precise measurement of $(\partial \rho_N/\partial C_2)_\mu$ is delicate. It requires $I(0)/C_2$ values (eq 12 in Material and Methods) obtained from homogeneous samples with no aggregation and negligible interparticle effects. They are sensitive to the

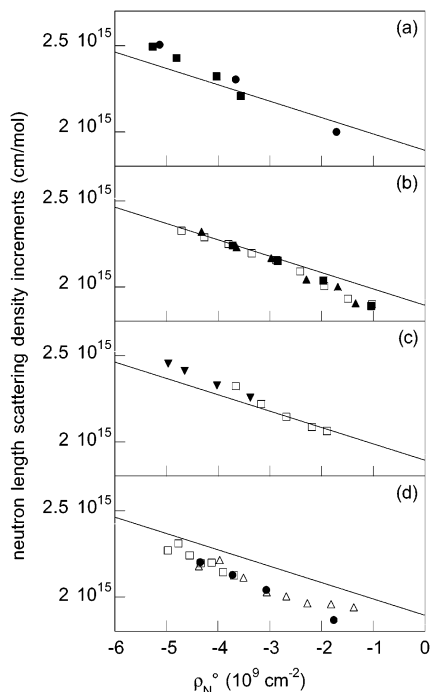


FIGURE 2: Neutron scattering density increments of *Hm* MalDH in various salts. They are plotted against the solvent neutron scattering length densities ρ_N^0 . The salt concentrations increase from left to right. Open symbols correspond to measurements performed at one protein concentration (3–6 mg/mL) and filled symbols to data extrapolated at infinite dilution. Panel A: squares, 0.2–1.3 M MgCl_2 ; circles, 0.25, 1, and 2 M MgSO_4 . Panel B: open squares, 1–5 M NaCl; filled squares, 2–5 M NaCl; triangles, 1.5–5 M NaCH_3CO_2 . Panel C: squares, 2–3.8 M KCl (data at pH 7 50 mM K Phos and room temperature from ref 34); triangles, 1–3.5 M KF. Panel D: squares, 1.4–4.5 M NH_4Cl ; triangles, 1.5–5 M $\text{NH}_4\text{CH}_3\text{CO}_2$; circles, 1–3 M $(\text{NH}_4)_2\text{SO}_4$. The line is $(b_2 - \rho_N^0 \bar{V}_2)$ and is calculated with $b_2 = 1.89 \cdot 10^{15}$ cm/mol from the amino acid composition of *Hm* MalDH and $\bar{V}_2 = 94\,500$ mL/mol.

background subtractions and have to be put on an absolute scale. Furthermore, the protein concentration C_2 has to be known in an absolute way. We checked the homogeneity of the material by gel filtration before the experiments. We verified by precisely weighted dilutions that the extinction coefficient of *Hm* MalDH is within the uncertainty (2%) for a variety of salt conditions. For about half the series of salts, the background subtraction was carefully checked and the forward intensities extrapolated at infinite protein dilution from a concentration series. As shown in Figure 2 for NaCl, this provided $(\partial\rho_N/\partial C_2)_\mu$ values similar to those measured at 5 mg/mL. On this Figure is also plotted data in KCl 2–3.8 M, at pH 7 and room temperature from (34). The published data at 20 °C, pH 7, for 1 M MgCl_2 (9) and 1 M NaCl (35) differ from ours data at pH 8.2, most probably because of the instability of *Hm* MalDH at pH 7.

The neutron scattering length density increment in SANS experiments, $(\partial\rho_N/\partial C_2)_\mu$, is related to the solvent scattering length density ρ_N^0 (eq 15). The values of $(\partial\rho_N/\partial C_2)_\mu$ are presented in Figure 2 as a function of ρ_N^0 , which increases with the salt concentration. Each panel corresponds to salts possessing a common cation: Mg^{2+} , Na^+ , K^+ , or NH_4^+ (panels a–d, respectively). The $(\partial\rho_N/\partial C_2)_\mu$ value decreases regularly with the salt concentration for all salts. On each panel is drawn a straight line corresponding to the neutron scattering length density increment $(b_2 - \rho_N^0 \bar{V}_2)$ calculated for

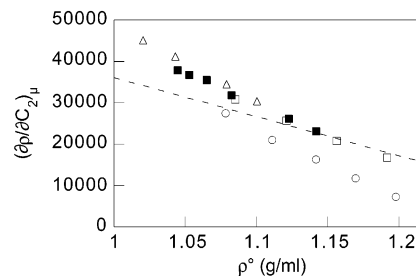


FIGURE 3: Density measurements of *Hm* MalDH in various salts. The density increments obtained after dialysis are plotted against the respective solvent densities. The salt concentration increases from left to right. Open squares, NaCl 2–5 M; filled squares, NaCH_3CO_2 1.5–3.5 M; triangles, MgCl_2 0.2–1.3 M; circles, $(\text{NH}_4)_2\text{SO}_4$ 1–3 M. The line is $(M_2 - \rho^0 \bar{V}_2)$ and is calculated with $M_2 = 130\,552$ g/mol and $\bar{V}_2 = 94\,500$ mL/mol inferred from the amino acid composition of *Hm* MalDH.

a hypothetical particle composed uniquely of the protein part (without consideration of the co-ions) and not perturbing the solvent. We used $\bar{V}_2 = 94\,500$ mL/mol (see below). The simple examination of the experimental data provides qualitative insights into the solvent interactions of *Hm* MalDH. It is obvious that data points essentially superimpose on each other for the same cation and also that the series of points corresponding to a common anion do not superimpose. This can be observed for Cl^- , which is common to all panels, or for CH_3CO_2^- and SO_4^{2-} , which were studied in combination with NH_4^+ and Na^+ , and NH_4^+ and Mg^{2+} , respectively. Thus, the values of $(\partial\rho_N/\partial C_2)_\mu$ depend essentially on the nature of the cation and not of the anion.

Mass Density Increments. The mass density increment, $(\partial\rho/\partial C_2)_\mu$, is related to the solvent density ρ^0 (eq 14). $(\partial\rho/\partial C_2)_\mu$'s in NaCl, NaCH_3CO_2 , MgCl_2 , and $(\text{NH}_4)_2\text{SO}_4$ are plotted against ρ^0 in Figure 3. As for Figure 2, the straight line $(M_2 - \rho^0 \bar{V}_2)$ corresponds to the hypothetical particle made up of protein only and with no solvent perturbation. Clearly, for each salt series, the density increments vary regularly as a function of the density. The mass density increments corresponding to the various salts do not superimpose, except for the series in NaCl and NaCH_3CO_2 , which overlap, in qualitative agreement with the SANS results.

Interpolation of \bar{V}_2 and $(\partial m_3/\partial m_2)_\mu$ from SANS and Mass Density Measurements. The experimental points of Figures 2 and 3 would be aligned for each type of salts in the case of an invariant particle of constant composition and total volume. Previously published mass and neutron scattering length densities of *Hm* MalDH in NaCl, pH 7, at 20 °C, in H_2O and D_2O (6, 14) were analyzed using the linear fitting of the data points. Using approximate constant values of \bar{V}_2 , \bar{V}_1 , \bar{V}_3 , it allowed to determine values for water and salt binding in the hypothesis of an invariant particle. In the present study, \bar{V}_2 and $(\partial m_3/\partial m_2)_\mu$ were experimentally obtained from SANS and mass density measurements performed in the same solvent (eqs 14 and 15). The results for MgCl_2 , NaCl, NaCH_3CO_2 , and $(\text{NH}_4)_2\text{SO}_4$ are reported in Table 1.

DISCUSSION

The Partial Molal Volumes \bar{V}_2 and \bar{V}_3 as a Function of Salt Type and Concentration. The partial molal volume of polyelectrolytes or salts is known to vary with the solvent composition and to increase with salt concentration. For

Table 1: Mass and Neutron Scattering Length Density Increments, Partial Molal Volumes, and Preferential Binding Parameters of *Hm* MalDH in the Presence of Various Salts^a

salt	C_3 (M)	m_3/m_1 (mol/mol)	ρ° (g/mL)	$(\partial\rho/\partial C_2)_\mu$ (10^3 g/mol)	ρ_N° (10^9 cm ⁻²)	$(\partial\rho_N/\partial C_2)_\mu$ (10^{15} cm/mol)	\bar{V}_2 (10^3 cm/mol)	$(\partial m_3/\partial m_2)_\mu$ (mol/mol)
NaCl	2	0.040	1.085	30.8 ± 0.5	-3.72	2.24 ± 0.05	93.9 ± 1.6	-38 ± 40
	3	0.059	1.121	25.7 ± 0.5	-2.85	2.15 ± 0.04	95.0 ± 1.6	-54 ± 40
	4	0.079	1.156	20.7 ± 0.5	-1.96	2.04 ± 0.04	95.5 ± 1.6	-90 ± 45
	5	0.101	1.192	16.7 ± 0.5	-1.04	1.89 ± 0.04	95.0 ± 1.6	-164 ± 45
NaCH ₃ CO ₂	1	0.019	1.045	38.0 ± 0.4	-4.33	2.33 ± 0.04	92.2 ± 1.3	5 ± 34
	1.5	0.030	1.065	34.9 ± 0.5	-3.65	2.24 ± 0.04	92.4 ± 1.5	-20 ± 30
	2	0.041	1.085	31.8 ± 0.5	-2.97	2.17 ± 0.04	93.4 ± 1.3	-30 ± 30
	2.5	0.053	1.104	29.0 ± 0.5	-2.30	2.07 ± 0.04	93.5 ± 1.3	-59 ± 35
	3	0.064	1.123	26.1 ± 0.6	-1.69	2.00 ± 0.04	94.8 ± 1.3	-78 ± 35
	3.5	0.078	1.142	23.2 ± 0.9	-1.00	1.91 ± 0.04	94.4 ± 1.6	-103 ± 36
MgCl ₂	0.2	0.004	1.020	45.1 ± 0.6	-5.27	2.49 ± 0.03	90.3 ± 1.6	64.5 ± 20
	0.5	0.009	1.043	41.3 ± 0.5	-4.81	2.43 ± 0.05	90.9 ± 2.4	48 ± 25
	1	0.018	1.079	34.6 ± 1.2	-4.03	2.32 ± 0.03	92.3 ± 1.6	23 ± 20
	1.3	0.024	1.100	30.4 ± 2.8	-3.57	2.21 ± 0.04	91.3 ± 3.6	-23 ± 25
(NH ₄) ₂ SO ₄	1	0.020	1.078	27.4 ± 0.5	-4.35	2.20 ± 0.04	95.5 ± 2.0	-46 ± 35
	1.5	0.031	1.111	21.0 ± 0.7	-3.72	2.13 ± 0.04	97.8 ± 2.7	-65 ± 35
	2	0.042	1.142	16.3 ± 0.5	-3.07	2.04 ± 0.04	98.4 ± 1.9	-90 ± 30
	2.5	0.055	1.170	11.8 ± 0.5	-2.42	1.95 ± 0.04	99.4 ± 1.7	-118 ± 34
	3	0.069	1.198	7.6 ± 0.5	-1.77	1.86 ± 0.04	100.0 ± 1.7	-147 ± 34

^a The solvent is characterized by the salt concentration C_3 (mol/L), the molar ratio between salt and water m_3/m_1 , and the mass and neutron scattering length densities, ρ° and ρ_N° , respectively. The values of the partial molal volumes \bar{V}_2 and preferential salt binding parameters $(\partial m_3/\partial m_2)_\mu$ of *Hm* MalDH were derived from the measurements of the mass and neutron scattering length density increments $(\partial\rho/\partial C_2)_\mu$ and $(\partial\rho_N/\partial C_2)_\mu$ (eqs 14 and 15, see the Material and Methods).

example, the partial specific volume of NaCl is given to be 16.6 mL/mol at infinite dilution (36), and we calculated it from density tables as 19.9, 21.3, 22.2, and 22.7 mL/mol at 2, 3, 4, and 5 M NaCl, respectively. Partial specific volumes of Na(CH₃CO₂) are 42.2 mL/mol at 1 M and 44.7 mL/mol at 3.5 M. For MgCl₂, the value at infinite dilution is 15.3 mL/mol and increases from 18.9 to 23.4 mL/mol between 0.2 and 1.3 M. Partial specific volume of (NH₄)₂SO₄ at infinite dilution can be estimated to be 49.5 mL/mol and increases from 63.2 to 76.2 mL/mol between 1 and 3 M salt. This is because the partial specific volume relates not only to the effective volume of the included species, but also to the changes in the volume of the solvent related to the addition of component. The same effects are observed for the partial specific volumes of nucleic acids, which increase with the solvent salt concentration (8, 20). It is admitted that the effect of water electrostriction is larger in diluted salt solution, which can be understood considering that in high salt most water molecules are already under the influence of a salt ion. Also, the formation of contact ion pairing is assumed to increase the values of the partial specific volumes (36, 37).

The partial molal volume \bar{V}_2 of *Hm* MalDH calculated from the scattering length and mass density increments vary mainly depending on the salt nature and increases with salt concentration (Figure 4). The partial specific volume of the polypeptide part can be calculated by two different ways, which both include the effect of charged groups on electrostriction: the first considers the specific volumes of the amino acids in solution, and the second uses the volumes of packed buried amino acids in protein crystals while adding a negative contribution of 10 and 18 Å³ by acidic and basic residues, respectively (38). The two procedures give very similar values of 92 800 and 93 100 mL/mol for the *Hm* MalDH polypeptide chain. Omitting the water electrostriction term in the latter procedure, a maximum value of 95 900 mL/mol is obtained. The partial molal volume of salt can

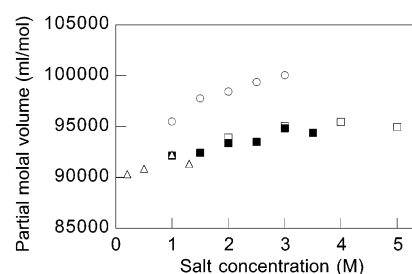


FIGURE 4: Partial molal volume \bar{V}_2 of *Hm* MalDH in various salts from SANS and density measurements. Triangle, MgCl₂; filled squares, NaCH₃CO₂; open squares, NaCl; circles, (NH₄)₂SO₄.

be decomposed into two additive contributions for anion and cation, \bar{V}_{anion} and \bar{V}_{cation} ; each of them can be divided into a positive molal volume—corresponding to an ionic radius 0.5 Å larger than one measured in crystals—and a negative electrostriction volume, the minimum of the sum of the two contribution being found at infinite dilution (36). The maximum and minimum values for \bar{V}_{cation} are given in Table 2 for selected cations. The calculated \bar{V}_2 of *Hm* MalDH with its co-ions for two limiting cases, infinite dilution in water (minimum value) and neglecting all electrostriction effects (maximum value), are compared to the experimental values in Table 2. The mean experimental values in 2–5 M NaCl, 1–3.5 M NaCH₃CO₂, and 1–3 M (NH₄)₂SO₄ are close to the mean calculated ones. Those in 0.2–1.3 M MgCl₂ are intermediate between the minimum and mean calculated values. Thus, the evolution, which is small but significant, and absolute values of \bar{V}_2 are compatible with expectations from the component composition.

The Preferential Binding Parameters Depend on Salt Type and Concentration. The values of the preferential binding parameters $(\partial m_3/\partial m_2)_\mu$ obtained in MgCl₂, NaCl, NaCH₃CO₂ and (NH₄)₂SO₄ clearly depend on the salt nature and concentration (Table 1 and Figure 5). The dissociation of the co-ions from the protein would lead to a negative contribution ($-E_3$, Donnan effect in eq 7) to $(\partial m_3/\partial m_2)_\mu$,

Table 2: Partial Molal Volumes of Ions and *Hm* MalDH^a

co-ion	\bar{V}_{cation} (mL/mol)		calculated \bar{V}_2 (10 ³ mL/mol)			experimental \bar{V}_2 (10 ³ mL/mol)
	min	max	min	max	mean	mean
Na ⁺	−6.6	8.2	92.0	97.3	94.6	94.9 (NaCl); 93.4 (NaCH ₃ CO ₂)
NH ₄ ⁺	12.4	23.3	94.9	99.6	97.3	98.2 ((NH ₄) ₂ SO ₄)
Mg ²⁺	−32	5.3	90.5	96.4	93.5	91.2 (MgCl ₂)

^a The calculated minimum and maximum values for the partial molal volumes of ions, \bar{V}_{cation} , and *Hm* MalDH component, \bar{V}_2 (corresponding to the polypeptide plus counterion contribution), take into account (min value) and omit (max value) electrostriction around the charged groups (see the text). The mean experimental values of the partial molal volumes of *Hm* MalDH component, \bar{V}_2 in the last column, obtained for each type of salt at different salt concentrations are taken from Table 1.

whose minimum values—for complete dissociation—are reported in Table 3. Contact ion pairing would decrease the absolute value of this negative contribution. The positive values for $(\partial m_3/\partial m_2)_\mu$ observed at low MgCl₂ (0.2–0.5 M) thus correspond to an excess of salt in the solvent perturbed by the protein, in addition to associated co-ions. The null values at 1–1.3 M MgCl₂ or 1–1.5 M NaCH₃CO₂ or NaCl indicate that there is no solvent redistribution when introducing the macromolecule with co-ions. The negative values found at all (NH₄)₂SO₄ concentrations, and also at high MgCl₂ and Na⁺ salts, correspond to an excess of water and/or to co-ions dissociation.

The Structural Interpretation in Terms of Strong Water and Salt Binding Sites. One value of $(\partial m_3/\partial m_2)_\mu$ corresponds to an infinite combination of N_1 and $(N_3 - E_3)$ values, N_1 and N_3 being the number of solvent water and salt molecules in the perturbed solvent, and E_3 the Donnan term arising from the co-ion protein dissociation. Here, eq 7 can be fitted linearly, considering the points for each salt type as linearly aligned in Figure 5. Thus, the solvation shell can be described as invariant, with values of N_1 and $(N_3 - E_3)$ that do not depend on the salt concentration, i.e., with two types of sites on the protein, one binding water very strongly and interacting negligibly with the salt and vice versa for the other (8, 22, 24). The deduced values of N_1 and $(N_3 - E_3)$ differ clearly from salt to salt (Table 3). $N_1 = 4100$ in MgCl₂ is larger by a factor of 2 compared to NaCl, NaCH₃CO₂, or (NH₄)₂SO₄ ($N_1 = 2000 \pm 200$). The number of salt molecules in the solvation shell is also strongly dependent on the salt nature, with $(N_3 - E_3)$ values ranging from 85 to 0 and decreasing in the order MgCl₂ > NaCl = NaCH₃CO₂ > (NH₄)₂SO₄. As was suggested by the raw experimental data (Figures 2 and 3), the salt and water binding are similar in NaCH₃CO₂ and NaCl. The approach cannot determine ion distribution or mechanisms of binding, so the distinction between incomplete dissociation of the polyelectrolyte and salt binding is artificial (see Figure 1). However, a positive value of the global salt binding $(N_3 - E_3)$ value indicates an accumulation of salt ions—related to the presence of the protein—that exceeds that of the counterions. If the case where the counterions did not dissociate from the protein in solution, the Donnan term would be null, and $(N_3 - E_3)$ would be related to additional ion binding.

Alternative Model with Solvent Exchangeable Binding Sites. Because the “invariant particle hypothesis model” is

not widely used and can appear as a restriction in the data analysis leading possibly to erroneous conclusions, we have used the alternative “solvent exchangeable binding sites model” of Schellman. The simple model consists of identical binding sites characterized by a water–ion equilibrium exchange constant. In this way, occupancy of the sites by water is larger at low salt, while at high salt, the sites are predominantly occupied by ions, the limit between “low” and “high” salt being related to the value of the equilibrium constant. Figure 6, panel A, shows the evolution of the salt binding parameters $(\partial m_3/\partial m_b)_\mu$ (which is $(\partial m_3/\partial m_2)_\mu$ normalized for one binding site) for a X⁺Y[−] ideal salt for different values of the equilibrium constant K_b . For $K_b = 0$, the site is always occupied by water, and the resulting $(\partial m_3/\partial m_b)_\mu$ is more and more negative when the salt concentration increases. $K_b = 2$ corresponds to a site that is solvent indifferent, with a constant null value of $(\partial m_3/\partial m_b)_\mu$, whatever the salt concentration. Increasing the value of K_b leads to the full occupancy of the site by an ion, with $(\partial m_3/\partial m_b)_\mu = 0.5$ salt per site. The model takes the nonideality of the solvent into account because it can result in drastic changes in the values of the preferential binding parameters. Figure 6, panel B, shows the values of f_\pm/f_1 that characterize the solvent nonideality for NaCl, NaCH₃CO₂, MgCl₂, and (NH₄)₂SO₄ solutions. On Figure 6, panel C, we demonstrate the effect of nonideality on the preferential salt binding parameters for hypothetical sites intrinsically indifferent to the solvent: $(\partial m_3/\partial m_b)_\mu$ would be zero if the salt were ideal. As expected, $(\partial m_3/\partial m_b)_\mu$ is increased when f_\pm/f_1 increases and decreases when f_\pm/f_1 decreases.

Because f_\pm/f_1 in NaCl, NaCH₃CO₂, or MgCl₂ increases with the salt concentration in the range of our measurements, one type of exchangeable binding site cannot model the positive values of $(\partial m_3/\partial m_2)_\mu$ at low salt and negative ones at higher salt measured for *Hm* MalDH (see Figure 5). Our experimental data cannot thus be described with only one type of solvent binding sites, and at least two types of sites are therefore required for halophilic MalDH in these salt conditions. We considered the model of N_1 water binding sites and N_b solvent-exchangeable binding sites, chosen from the invariant particle model, to determine the minimum values for the exchangeable equilibrium constant K_b in the mole fraction scale (Table 3). They are by 2 or 3 orders of magnitude larger than the K_b values of 2 or 3 corresponding to chemical indifference for water and ions. In contrast, in (NH₄)₂SO₄, the solvent nonideality decreases significantly the effect of the true affinity for the ions and in a more extent at high salt (with decreasing values of f_\pm/f_1). In this salt, the solvent binding sites with a low affinity for salt are indistinguishable from water binding sites. With a small Donnan contribution ($E_3 = 10$), our data can be fitted considering one type of 2300 independent solvent exchangeable sites with $K_d = 3$ that corresponds to chemical indifference for ions or water. Restricting our analysis to very simple models, i.e., with a minimum of type of solvent binding sites, the introduction of exchangeable binding sites and of solvent nonideality effects thus does not change the essential conclusions found using the invariant particle hypothesis.

Anions Stabilize Hm MalDH through a Limited Number of Strong Binding Sites. The density increments presented

Table 3: Structural Interpretation of the Preferential Binding Parameters $(\partial m_3/\partial m_2)_\mu$ of *Hm* MalDH in Terms of Water and Salt Binding Sites, and Concentration of the perturbed solvent^a

salt	invariant particle model		solvent exchange model with solvent nonideality	max Donnan term, $-E_3$ (mol/mol)	perturbed solvent concentration (M)
	N_1 (mol/mol)	$N_3 - E_3$ (mol/mol)			
MgCl ₂	4100	85	$N_1 = 4100, N_b = 255, QK_b = 8000$	-26	1.1–1.4
NaCl	2100	55	$N_1 = 2100, N_b = 115, QK_b = 200$	-78	1.5–3.4
NaCH ₃ CO ₂	1800	40	$N_1 = 1800, N_b = 80, QK_b = 800$	-78	1.1–3.1
(NH ₄) ₂ SO ₄	2100	0	$E_3 = 10, N_b = 2300, QK_b = 3$	-52	<0–1.2

^a N_1 and N_3 are the numbers of water and salt binding sites on *Hm* MalDH. E_3 is the Donnan term related to the dissociation of the positive co-ions associated to the macromolecular compound. The values of the invariant particle model are obtained from the linear fit of $(\partial m_3/\partial m_2)_\mu$ as a function of m_3/m_1 (eq 7). In the solvent exchange model, N_b is the number of sites exchanging solvent water and ion, with an equilibrium exchange constant QK_b defined in a mole fraction scale. A number N_3 of salt binding sites corresponds to $N_b = 2N_3$ ion binding site in NaCl and NaCH₃CO₂ and $N_b = 3N_3$ in MgCl₂ and (NH₄)₂SO₄. A value of $QK_b = 2$ in NaCl and NaCH₃CO₂ and of $QK_b = 3$ in MgCl₂ and (NH₄)₂SO₄ would correspond to chemical in difference for water and ions. The solvent-exchange model considers the solvent nonideality. The minimum value for the concentration of the perturbed solvent (last column) is the solvent concentration for which we measured $(\partial m_3/\partial m_2)_\mu = 0$, and the maximum value is that for which $(\partial m_3/\partial m_2)_\mu = -E_3$.

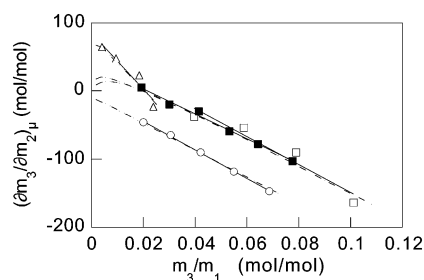


FIGURE 5: Modeling the preferential salt binding parameters of *Hm* MalDH in various salts. Preferential binding parameters $(\partial m_3/\partial m_2)_\mu$ are plotted against (m_3/m_1) , the molar ratio between salt and water of the solvent. They were measured in MgCl₂ (triangles), NaCl (open squares), NaCH₃CO₂ (filled squares), and (NH₄)₂SO₄ (circles). The numbers of molecules of water and salt, N_1 and $(N_3 - E_3)$, associated to the protein component in the model of an invariant particle are determined from linear fitting (continuous lines). N_3 is the number of solvent salt associated, and E_3 is the Donnan exclusion term. The dashed lines model the data with solvent binding sites exchanging water and solvent ions and take into account the effect of solvent nonideality. The numerical values obtained from the fit are reported in Table 3.

in Figures 2 and 3 are very similar for salts with a common cation. It suggests that the solvent interactions as globally weighted depend mainly on the nature of the cation. Indeed, the solvent interactions quantified in NaCl and NaCH₃CO₂ are very similar, and very different from those determined in the presence of Mg²⁺ or NH₄⁺ salts. The anions tested here modulate the solvent interactions perhaps at very high salt, as suggested for the ammonium salts (Figure 2, panel d). One counterexample is a previous measurement in 1.5 M K-phosphate, for which preferential hydration was measured (9), which differs from the measurements in KCl and KF presented in Figure 2. The negligible effect of anions on the values of the preferential binding parameter is unexpected if we consider previous works on nonhalophilic proteins. The preferential hydration of nonhalophilic proteins in 1 M salt is described to increase in the order of Cl⁻ < CH₃CO₂⁻ < SO₄²⁻ by Timasheff et al. (39). It is generally admitted that anions of high charge density (SO₄²⁻, F⁻) are the most efficient to stabilize the folded form of proteins according to the Hofmeister series because they increase the surface tension of the solvent (cations having a smaller effect on surface tension, 40). This corresponds to a relative accumulation of water around the protein, which destabilizes the macromolecule state with the largest exposed surface,

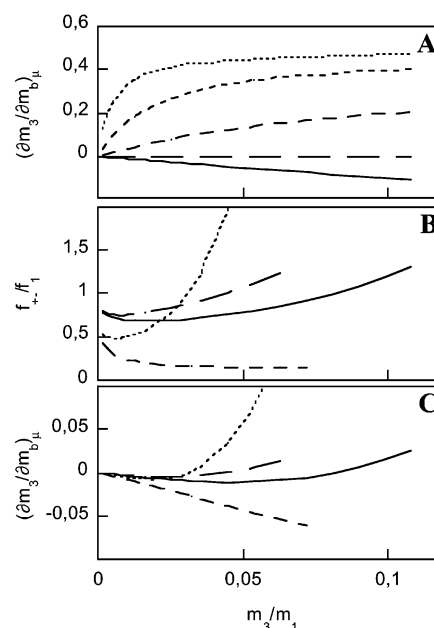


FIGURE 6: Evolution of $(\partial m_3/\partial m_b)_\mu$ in the model of N_b identical solvent-exchangeable binding sites and considering the salt solution nonideality. A: Evolution of the preferential salt binding parameters normalized for one binding site $(\partial m_3/\partial m_b)_\mu$ against (m_3/m_1) , the molar ratio between salt and water of the solvent, in the case of an ideal monovalent solvent salt. K_b , the water-ion exchangeable equilibrium constant defined in the mole fraction scale, is 0, 2, 10, 50, and 200 (from the continuous line to the dotted line). B: Values of the ratios of the activity coefficients defined in the mole fraction scale of ion, f_{\pm} , and water, f_1 , for NaCl (—), NaCH₃CO₂ (---), (NH₄)₂SO₄ (---), and MgCl₂ (···). C: Evolution of $(\partial m_3/\partial m_b)_\mu$ against (m_3/m_1) for $K_b = 2$ in NaCl (—), $K_b = 2$ in NaCH₃CO₂ (---), $K_b = 1.890$ in (NH₄)₂SO₄ (---), and $K_b = 1.899$ in MgCl₂ (···). The values of K_b were chosen in such a way that, in the absence of solvent nonideality, $(\partial m_3/\partial m_b)_\mu$ would be null (see the text).

i.e., the unfolded protein. This general effect is masked for *Hm* MalDH.

The small effect of anions on the measured global solvent interactions of *Hm* MalDH might appear to be logical in view of the very acidic character of the halophilic protein. However, both anions and cations were found to determine *Hm* MalDH stability (15). It was found that the salt transition between folded and unfolded forms was negligibly related to the surface tensions of the solution, which determine a nonspecific mechanism of stabilization. This has suggested

that some specific interactions between anions and folded *Hm* MalDH would be required to stabilize it. Relatively strong binding sites were suggested from the fact that in the presence of anions stabilizing *Hm* MalDH at low concentration (below the molar range), the impact of the type of cations was limited (and vice versa) (15). The small variation of the preferential binding parameters as a function of the anions demonstrates that they act on protein stability essentially through strong binding to a limited number of sites, specific of the folded form of *Hm* MalDH. High-resolution crystallographic studies show indeed a few binding sites for ions, which are anions and cations in about the same proportion, despite the acidic character of the protein. In the *Hm* MalDH structure solved at 2.6 Å, extended salt bridge clusters at the dimer-dimer interface appear as “locked” in by four bound chloride ions (11).

The Solvent Interactions of Hm MalDH Compared to Those of Other Proteins. In NH_4^+ salts, *Hm* MalDH can be described with water binding sites only, or with sites chemically indifferent to water and salt with the net hydration resulting from solvent nonideality. This evolution of $(\partial m_3/\partial m_2)_\mu$ —with negative values decreasing nearly linearly with the salt concentration—is commonly observed for macromolecules in the presence of cosolvent for which they have no or small affinity, such as, for example, osmoprotectants (41). In contrast, in NaCl, NaCH_3CO_2 or MgCl_2 , the solvation shell of *Hm* MalDH contains a large number of salt molecules with a high local salt concentration (about 1–1.5 M) in addition to the co-ions introduced by the macromolecule, corresponding, as a whole, to 1.4 M MgCl_2 or 3.1–3.4 M NaCH_3CO_2 or NaCl (Table 3). Salt binding on the halophilic protein is obviously quantitatively exceptional in front of nonhalophilic ones. However, there are evidences of binding sites for ions on nonhalophilic proteins. Bovine serum albumin and β -lactoglobulin have been described to bind NaCl (22, 42). The close to zero or slightly positive values of $(\partial m_3/\partial m_2)_\mu$ for bovine serum albumin, β -lactoglobulin, and lysozyme in low MgCl_2 at the isoelectric pH indicate salt binding when the proteins are negatively charged (43). Our analysis suggests that the ionic binding sites of the highly negatively charged folded form of *Hm* MalDH are saturated at the lowest salt concentration of our measurements, which corresponds approximately to the concentration required for the stabilization of the folded form. The preferential hydration observed above 1 M can be modeled as the result of specific binding sites for water. The data does not give insight on the origin of the water accumulation at the interfaces. A nonspecific mechanism of hydration as that described from the surface tension effect would not be discernible to the specific one resulting from water binding sites. Thus, apart from the few effects of the solvent anions, the solvent interactions of the halophilic protein differ from a nonhalophilic one only by the number and strength of the Na^+ and Mg^{2+} binding sites.

The Stabilizing Effect of Salts Can Be Related to Water or Ion Binding. From thermodynamics, the state of a protein—e.g., folded or unfolded—interacting more efficiently with salt and less efficiently with water is stabilized when increasing the salt concentration (44–46). If the sign of the preferential salt binding parameters and the folding state of the protein are not correlated, the effect of a cosolvent stabilizing the folded form is always related to its more larger

affinity exclusion—or less exclusion affinity—for the folded form when compared to the unfolded one. For a stabilizing cosolvent, the preferential binding parameter $(\partial m_3/\partial m_2)_\mu$ is more positive for the folded form, whatever its absolute value or sign (47). The present study addresses the halophilic protein in its native state. The differences in $(\partial m_3/\partial m_2)_\mu$ regarding the type of cation are easily related to the presence of negatively charged binding sites. We recall that *Hm* MalDH tetramer has an excess of 156 negative charges, whose corresponding carboxylates are distributed on the protein surface (48). We measure a number—and possibly affinity—of salt binding sites increasing in the order $\text{NH}_4^+ < \text{Na}^+ < \text{Mg}^{2+}$. It is interesting to note that two very different mechanisms arising from weak interactions with the solvent can combine for the stabilization of the folded protein at high salt. Hydration of the protein stabilizes the folded form—the unfolded one having a larger exposed surface area—in a more efficient way at higher salt. Salt binding sites on the folded form will also stabilize it when increasing the salt. Thus, in $(\text{NH}_4)_2\text{SO}_4$, we measure preferential hydration for the folded form at all tested salt concentrations (above 1 M), with about 2000 sites binding water, which could weakly exchange for salt ions. In this salt, cold unfolding was evidenced and interpreted in term of stabilization by hydrophobic effect (14). Despite the fact that it could be related to various fundamental processes such as dehydration in hydrogen bond or salt bridge formation (49), cold unfolding correlates here with water excess on the folded protein surface, the denatured form being obligatory hydrated to an even larger extent. In NaCl, NaCH_3CO_2 , or MgCl_2 , ionic binding sites on the folded form are evidenced, whose affinity is sufficient to bring them to saturation at the minimum salt concentration required for the protein stabilization. It is reasonable to consider that some of these binding sites are strong and can be detected by high-resolution crystallography. On the other hand, most of them are weak and disordered. The weak sites vary in number with the salt type and allow the native *Hm* MalDH stabilization only at relatively high salt. Because increasing these salts stabilize the folded protein, the unfolded form possesses more water binding sites or ionic binding sites in fewer number or affinity. The close location of the carboxylates on the surface of the folded protein could strengthen the weak binding of cations and explain both the exceptional solvation measured here and their stabilizing efficiency measured in a previous work (15). The relative efficiency of the cations for *Hm* MalDH stabilization, $\text{Ca}^{2+} \approx \text{Mg}^{2+} > \text{Li}^+ \approx \text{NH}_4^+ \approx \text{Na}^+ > \text{K}^+ > \text{Rb}^+ > \text{Cs}^+$, was discussed in the framework of ion pair selectivity rules proposed by Collins (40), which favored the interactions between water-ordering ions. The kosmotropic character is related to the charge density of the solvent cations and could be enhanced for the carboxylates exposed at the surface of the folded protein due to their closed localization, when compared to those of the unfolded form.

CONCLUSION

In a review on halophilic adaptation (1), we defined a halophilic protein in an operational way, as a protein extracted from a halophilic microorganism that requires at least 2.5 M NaCl in the medium for optimal growth. All proteins—even if halophilic—are different. Dihydrofolate

reductase from *H. volcanii* (*Hv* DHRF) is not particularly acidic compared to nonhalophilic analogues (50). *Hm* MalDH presents extended salt bridges that do not exist in *Hm* 2Fe–2S ferredoxin (10) or *Hv* DHRF (51). Also, the salt requirements of these proteins for optimum stability or activity are very different. Even the main biophysical characteristic of halophilic proteins, i.e., the salt requirement for stability, can be questioned since the addition of cofactors for *Hm* MalDH (unpublished results) or pH variations in the case of *Hv* DHRF (50) can drastically shift unfolding toward lower salt. It is an open question how the in vitro conditions compare to the complex intracellular crowded cytoplasm. The biochemical machinery in the extreme halophilic *archae* is in general similar to that of other organisms, with some specific cellular adaptation features, such as distinctive lipid composition (52) or response systems to low salt stress (53). Therefore, understanding halophilic behavior is equivalent to understanding how biochemical reactions can take place in the usual way in the presence of high salt, which is of course a difficult question. Also, the linkage of stability and protein–solvent interactions is in general difficult because the involved energies are not large, as a whole, compared to the sums of the energies corresponding to the disruption and contacts made.

Because salt remains central to the question of the halophilic adaptation of molecular mechanisms, our strategy was to compare the effects of several salts on the behavior of one halophilic protein (*Hm* MalDH). To what extent are the effects of salts on this protein specific to its halophilic character? A previous work on the relative stability of this enzyme (15) concluded that interactions between ions— anions and cations—and this protein in the folded form were specifically important to stabilize the folded form. Of course, the addition of specific and nonspecific effects of salts was observed and hard to discriminate. In the present paper, we characterize the solvent binding of *Hm* MalDH. We used complementary mass density and small neutron scattering measurements, taking into account the effects of weak protein–protein interactions, which, with the solvent interactions, modulate the solution scattering properties. The expected evolution of the partial specific volume values as a function of salt type and concentration is a good control of the quality of our result.

Because salt binding parameters do not depend on the nature of the solvent salt anion, for the salts investigated here, our results clearly demonstrate that anions act on protein stability through a small number of binding sites. In addition, our results show bound salt and water values that depend strongly on the cation of the salt and are exceptional compared to those described for nonhalophilic proteins, in Na^+ and Mg^{2+} salts, for example. We were careful to obtain accurate data and to interpret them as a function of salt concentrations by using the “invariant particle hypothesis model” and also the alternate “solvent exchangeable binding sites model” of Schellman (23). The “invariant particle hypothesis model” is not widely used and could appear as a restriction in the data analysis leading possibly to erroneous conclusions (but we found similar results with the two approaches). Different amounts of water and salt solvate the folded *Hm* MalDH, depending of the type of cation present. The number of solvating water molecules is higher in magnesium salts than in sodium or ammonium ones (4100

against 2000 mol per *Hm* MalDH tetramer). The number of salt molecules associated to the particle, from salt binding and Donnan exclusion (two not separated effects) decreases from 85 in magnesium chloride to about 50 in sodium chloride or acetate and 0 in ammonium sulfate salts.

In what extend are the solvation values of *Hm* MalDH exceptional? Salt binding has been found also for nonhalophilic proteins (which display also a large diversity of behavior). We conclude that the solvation of halophilic proteins is quantitatively but not qualitatively different from nonhalophilic ones. Specific weak binding of cations on the folded form of *Hm* MalDH and nonspecific hydration have the same effect on protein stabilization. At high salt, the former stabilizes the folded form and the latter destabilizes to a larger extent the unfolded form. Information concerning *Hm* MalDH stabilization is thus obtained combining the present results on protein solvation with its high-resolution structure and stability measurements as a function of salt and/or temperature. In ammonium sulfate, cold unfolding was interpreted in terms of the hydrophobic effect, which is in qualitative agreement with our finding of a solvation shell composed of just water. In sodium and magnesium salts, the affinity of ionic binding sites—some are seen in the high-resolution structures—is sufficient to bring them at saturation when the protein is stable, above 0.2 M MgCl_2 , 1 M NaCl at 4°C, pH 8. Obviously, they participate in protein stabilization. The close location of the carboxylates on the surface of the folded very acidic *Hm* MalDH could strengthen the weak binding of cations and also explain their stabilizing efficiency.

In the present paper, we confirm the exceptional solvation properties of *Hm* MalDH. Protein–solvent interactions modulate through different mechanisms protein stabilization at high salt. However, the challenges for the halophilic proteins in their crowded and salty cytoplasm are not only stability but also flexibility and solubility, which are required for biological function and activity. The flexibility of *Hm* MalDH was investigated in KCl and NaCl, in the presence of H_2O and D_2O , and a higher stability was associated with increased resilience (54). On the other hand, salts in the molar range are well-known to affect strongly protein solubility (55). In the companion paper (31), we evaluate how weak *Hm* MalDH–*Hm* MalDH interactions depend on solvent composition and emphasize the effect of solvation on protein solubility.

ACKNOWLEDGMENT

Thanks are due to R. May and P. Timmins (ILL) for fruitful discussions and help with the neutron experiments.

REFERENCES

1. Madern, D., Ebel, C., and Zaccai, G. (2000) *Extremophiles* 4, 91–98.
2. Mevarech, M., Frolow, F., and Gloss, L. M. (2000) *Biophys. Chem.* 86, 155–164.
3. Madern, D., Pfister, C., and Zaccai, G. (1995) *Eur. J. Biochem.* 230, 1088–1095.
4. Ng, W. V., Kennedy, S. P., Mahairas, G. G., Berquist, B., Pan, M., Shukla, H. D., Lasky, S. R., Baliga, N. S., Thorsson, V., Sbrogna, J., Swartzell, S., Weir, D., Hall, J., Dahl, T. A., Welti, R., Goo, Y. A., Leithauser, B., Keller, K., Cruz, R., Danson, M. J., Hough, D. W., Maddocks, D. G., Jablonski, P. E., Krebs, M. P., Angevine, C. M., Dale, H., Isenbarger, T. A., Peck, R. F., Pohlshroder, M., Spudich, J. L., Jung, K. W., Alam, M., Freitas,

- T., Hou, S., Daniels, C. J., Dennis, P. P., Omer, A. D., Ebhardt, H., Lowe, T. M., Liang, P., Riley, M., Hood, L., and DasSarma, S. (2000) *Proc. Natl. Acad. Sci. U.S.A.* 97, 12176–12181.
5. Ebel, C., Guinet, F., Langowski, J., Urbanke, C., Gagnon, J., and Zaccai, G. (1992) *J. Mol. Biol.* 223, 361–371.
6. Bonneté, F., Ebel, C., Eisenberg, H., and Zaccai, G. (1993) *J. Chem. Soc., Faraday Trans.* 89, 2659–2666.
7. Ebel, C., Altekar, W., Langowski, J., Urbanke, C., Forest, E., and Zaccai, G. (1995) *Biophys. Chem.* 54, 219–227.
8. Kernel, B., Zaccai, G., and Ebel, C. (1999) *Prog. Colloid Polym. Sci.* 113, 168–175.
9. Zaccai, G., Cendrin, F., Haik, Y., Borochov, N., and Eisenberg, H. (1989) *J. Mol. Biol.* 208, 491–500.
10. Frolov, F., Harel, M., Sussman, J. L., Mevarech, M., and Shoham, M. (1996) *Nat. Struct. Biol.* 3, 452–458.
11. Richard, S. B., Madern, D., Garcin, E., and Zaccai, G. (2000) *Biochemistry* 39, 992–1000.
12. Klement, R., Soumpasis, D. M., and Jovin, T. M. (1991) *Proc. Natl. Acad. Sci. U.S.A.* 88, 4631–4635.
13. Feig, M., and Pettitt, B. M. (1999) *Biophys. J.* 77, 1769–1781.
14. Bonneté, F., Madern, D., and Zaccai, G. (1994) *J. Mol. Biol.* 244, 436–447.
15. Ebel, C., Faou, P., Kernel, B., and Zaccai, G. (1999) *Biochemistry* 38, 9039–9047.
16. Madern, D., and Zaccai, G. (1997) *Eur. J. Biochem.* 249, 607–611.
17. Sears, V. F. (1992) in *International Tables for Crystallography* (A. J. C., W., Ed.) pp 383–391, Kluwer Academic Publishers, Dordrecht.
18. Tanford, C. (1961) *Physical Chemistry of Macromolecules*, Wiley, New York.
19. Eisenberg, H. (1976) *Biological macromolecules and Polyelectrolytes in Solution*, Clarendon Press, Oxford.
20. Cohen, G., and Eisenberg, H. (1968) *Biopolymers* 6, 1077–100.
21. Tardieu, A., Vachette, P., Gulik, A., and Le Maire, M. (1981) *Biochemistry* 20, 4399–4406.
22. Eisenberg, H. (1994) *Biophys. Chem.* 53, 57–68.
23. Schellman, J. A. (1990) *Biophys. Chem.* 37, 121–140.
24. Schellman, J. A. (1994) *Biopolymers* 34, 1015–1026.
25. Schellman, J. A., and Gassner, N. C. (1996) *Biophys. Chem.* 59, 259–275.
26. Robinson, R. A., and Stokes, R. H. (1959) *Electrolyte Solutions*, 2nd ed., Butterworths, London.
27. Cendrin, F., Chroboczek, J., Zaccai, G., Eisenberg, H., and Mevarech, M. (1993) *Biochemistry* 32, 4308–4313.
28. Lindner, P., May, R. P., and Timmins, P. A. (1992) *Phys. B* 180 & 181, 967–972.
29. Guinier, A., and Fournet, G. (1955) *Small-angle Scattering of X-rays*, Wiley, New York.
30. Ebel, C., Faou, P., and Zaccai, G. (1999) *J. Cryst. Growth* 196, 395–402.
31. Costenaro, L., Zaccai, G., and Ebel, C. (2002) *Biochemistry* 41, 13245–13252.
32. Eisenberg, H. (1981) *Q. Rev. Biophys.* 14, 141–172.
33. Jacrot, B., and Zaccai, G. (1981) *Biopolymers* 20, 2413–2426.
34. Calmettes, P., Eisenberg, H., and Zaccai, G. (1987) *Biophys. Chem.* 26, 279–290.
35. Zaccai, G., Bunick, G. J., and Eisenberg, H. (1986) *J. Mol. Biol.* 192, 155–157.
36. Horvath, A. L. (1985) *Handbook of Aqueous Electrolyte Solutions. Physical Properties, Estimation and Correlation Methods*, Ellis Horwood Limited Chichester, New York.
37. Millero, F. J. (1969) *Limnol. Oceanogr.* 14, 376–385.
38. Harpaz, Y., Gerstein, M., and Chothia, C. (1994) *Structure* 2, 641–649.
39. Timasheff, S. N. (1993) *Annu. Rev. Biophys. Biomol. Struct.* 22, 67–97.
40. Collins, K. D. (1997) *Biophys. J.* 72, 65–76.
41. Courtenay, E. S., Capp, M. W., Anderson, C. F., and Record, M. T., Jr. (2000) *Biochemistry* 39, 4455–4471.
42. Arakawa, T., and Timasheff, S. N. (1987) *Biochemistry* 26, 5147–5153.
43. Arakawa, T., and Timasheff, S. N. (1984) *Biochemistry* 23, 5912–5923.
44. Timasheff, S. N. (1998) *Adv. Protein Chem.* 51, 355–432.
45. Record, M. T., Jr., Zhang, W., and Anderson, C. F. (1998) *Adv. Protein Chem.* 51, 281–353.
46. Parsegian, V. A., Rand, R. P., and Rau, D. C. (2000) *Proc. Natl. Acad. Sci. U.S.A.* 97, 3987–3992.
47. Xie, G., and Timasheff, S. N. (1997) *Protein Sci.* 6, 222–232.
48. Dym, O., Mevarech, M., and Sussman, J. L. (1995) *Science* 267, 1344–1346.
49. Makhataдзе, G. I., and Privalov, P. L. (1995) *Adv. Protein Chem.* 47, 307–425.
50. Bohm, G., and Jaenicke, R. (1994) *Protein Eng.* 7, 213–220.
51. Pieper, U., Kapadia, G., Mevarech, M., and Herzberg, O. (1998) *Structure* 6, 75–88.
52. Kates, M. (1993) in *New Comprehensive Biochemistry* (M. Kates, Kushner, and Matheson, Eds.) pp 261–295, Elsevier, Amsterdam.
53. Franzetti, B., Schoehn, G., Ebel, C., Gagnon, J., Ruigrok, R. W., and Zaccai, G. (2001) *J. Biol. Chem.* 276, 29906–29914.
54. Tehei, M., Madern, D., Pfister, C., and Zaccai, G. (2001) *Proc. Natl. Acad. Sci. U.S.A.* 98, 14356–14361.
55. Von Hippel, P., and Schleich, T. (1969) in *Structure of Biological Macromolecules*, pp 417–575, Marcel Dekker Inc., N. Y.

BI0258290